Available online at www.sciencedirect.com
SCIENCE DIRECT®
Journal of Nuclear Materials 324 (2004) 165–176
journal of nuclear materials
www.elsevier.com/locate/jnucmat

Comments on the stability of zirconium hydride phases in Zircaloy

L. Lanzani [a,*], M. Ruch [b]

[a] *Materials Department, Centro Atomico Constituyentes, Comision Nacional de Energia Atomica, Av. Libertador 8250, 1429 Buenos Aires, Argentina*

[b] *Non Destructive and Structural Testing Department, Centro Atomico Constituyentes, Comision Nacional de Energia Atomica, Av. Libertador 8250, 1429 Buenos Aires, Argentina*

Received 16 June 2003; accepted 22 September 2003

Abstract

As part of a project for the non-destructive assessment (NDA) of hydrogen content in Zircaloy-4 tubing, a series of Zircaloy-4 slabs were submitted to accelerated corrosion autoclaving tests in 1 M LiOH, in order to obtain thick oxide layers and high hydrogen pickup. These specimens were used as primary standards for oxide thickness eddy currents (ET) NDA and as secondary standards for hydrogen content ET-NDA. Specimen preparation and the non-destructive studies have been reported elsewhere. In the present work, the evolution of the hydride phases in these autoclaved Zircaloy-4 slabs was studied over a period of about 3 years, and the results are compared to those from other authors who worked with zirconium, Zircaloy or zirconium–niobium alloys. A revision of the literature on zirconium hydrides up to 2002 is presented.

1. Introduction

The Zr–H system has been studied by many authors over the last 50 years or more, because hydrogen pickup is responsible for embrittlement and fracture of zirconium alloys used in structural components of nuclear reactors.

The phase diagram of the binary system Zr–H proposed by Beck in 1962 [1] consists of two allotropic forms of zirconium, α-Zr (hcp) and β-Zr (bcc); two stable hydride phases, δ-hydride (fcc) and ε-hydride (fct), and one metastable phase, γ-hydride (fct), which can exist at the lower temperatures in the $(\alpha + \delta)$ phase region. There is an eutectoid reaction $\beta \rightarrow \alpha + \delta$ at 550 °C and 41 at.% H.

Northwood discussed this diagram in his 1983 review [2], in which he analyzes results from many authors, some of them proposing that the γ-phase is an equilibrium phase, formed by a peritectoid reaction at about 255 °C [3]. Northwood accepts however Beck's diagram and the metastability of the γ-phase based upon experimental evidence. The Zr–H phase diagram was further reviewed by Zuzek and coworkers, in two papers published in 1990 and 2000, respectively [4,5]. The earlier revision included literature up to 1986 while the more recent one, up to 1995.

In the 1990 paper [4], the metastability of the γ-hydride is accepted and, as regards the eutectoid composition, a slightly lower hydrogen content than Beck's is proposed [4], while in the 2000 paper [5], experimental evidence from Bashkin and coworkers of the peritectoid $(\alpha + \delta) \rightarrow \gamma$ reaction at 286 °C and 50 at.% H is presented [6,7].

Mishra et al. [3], Zuzek et al. [5] and Bashkin [6,7] actually state that in the Zr–H system, γ-hydride is an equilibrium phase which is stable below 250–280 °C and atmospheric pressure. More recent papers by Root and coworkers [8,9] however report having observed by neutron diffraction a reversible δ/γ transformation at

* Corresponding author.
E-mail addresses: lanzani@cnea.gov.ar (L. Lanzani), ruch@cnea.gov.ar (M. Ruch).

0022-3115/$ - see front matter © 2003 Elsevier B.V. All rights reserved.
doi:10.1016/j.jnucmat.2003.09.013

about 180 °C in Zr–2.5%Nb. This transformation was observed during heating and cooling experiments, while continued γ-precipitation occurred during long term room temperature (RT) aging.

The stability of the γ-hydride has been discussed by many authors. In particular, Northwood [10] submitted samples of Zr 98.75% (which initially contained up to 27.5 at.% H in the form of δ-hydride) to heat treatments (HT) at 220°–240 °C for 2200 h and found no evidence of a $\delta \rightarrow \gamma$ transformation. These results might rule out those by Mishra and Bashkin, but provide no evidence of a transformation at 180 °C. Hence, in order to investigate the 180 °C phenomena, the evolution of δ-hydride in Zircaloy-4 at RT and during aging at about 150 °C and further RT-aging has been studied in the present work. The starting materials were autoclaved Zircaloy-4 specimens containing only δ-hydrides, which had been prepared by the authors [11,12]. The phases present after all stages were characterized by X-ray diffraction (XRD) of the massive specimens. Besides, a review of the literature on zirconium hydrides up to 2002 is presented [3,6–10,13–26].

2. Experimental details

2.1. Material

The 50 mm long specimens were cut from a 20 mm wide, 1.1 mm thick Zircaloy-4 strip with a hydrogen content of 5 to 7 wt ppm. The strip was supplied by FAESA-Argentina. The microstructure of the alloy consisted of equiaxed α-grains (grain size about 50 μm) and uniformly distributed $Zr(Fe/Cr)_2$ precipitates (diameter of less than 0.5 μm). The typical composition of Zircaloy-4 is Sn: 1.20–1.70 wt%; Fe: 0.18–0.24 wt%; Cr: 0.07–0.13 wt%; O ≈ 1400 wt ppm; Zr and impurities to balance.

2.2. Corrosion tests and heat treatment

The specimens were submitted to a experimental sequence which spanned more than 3 years and included corrosion tests, HT, RT-aging and several XRD studies. This sequence is summarized in Table 1.

Hydrogen had been introduced into the specimens by autoclave accelerated corrosion tests in LiOH, a method which produces thick layers of ZrO_2 on the surface of the samples and a high hydrogen pickup (about 70%) [11,12].

The corrosion tests were performed in a static stainless steel autoclave with a titanium liner, in a 1M LiOH solution at (340 ± 3) °C and (13.6 ± 0.1) MPa. The extent of the corrosion reaction was controlled through the exposure time. Prior to the test, the specimens had been abraded with emery paper down to 1200 mesh, rinsed in doubly distilled water, dried with acetone, measured and weighed. Some specimens received several autoclaving steps in order to homogenize the hydride distribution. After these tests, two pieces were cut from the autoclaved specimens for metallography and for the measurement of hydrogen concentration in a LECO™ hydrogen analyzer. The experimental procedures and results have been reported elsewhere [12].

The hydrides were studied by XRD on the larger portion of the specimens, after removal of the oxide layer by abrasion with emery paper down to 2500 mesh. In order to avoid hydride alterations induced by chemical etching [13], this procedure was not performed on these samples.

XRD experiment 'a' was made a few days after autoclaving. After 24 months RT-aging, four out of

Table 1
Scheme of the experimental sequence the material was submitted to

Experimental sequence:
Hydriding by autoclaving tests in 1 M LiOH at (340 ± 3) °C and (13.6 ± 0.1) MPa
Autoclave cooling, $v_c \approx 0.5$ °C/min. Single or multiple step treatment
Removal of oxide layer by abrasion with emery papers. *No chemical etching*
X-ray diffraction study of hydrides, experiment "a", at 1 s/step, $20° \leqslant 2\theta \leqslant 130°$

⇓

19 months storage at room temperature (RT)
X-ray diffraction experiment "b", at 1 s/step, $20° \leqslant 2\theta \leqslant 130°$

⇓

5 months storage at RT
Heat treatment (HT) 2212 h at (148 ± 1) °C
Furnace cooling, $v_c \approx 1$ °C/min
X-ray diffraction experiment "c", at 1 s/step, $20° \leqslant 2\theta \leqslant 130°$

⇓

3 months storage at RT
X-ray diffraction, experiment "d", at 2 s/step, $20° \leqslant 2\theta \leqslant 80°$

⇓

2 months storage at RT
X-ray diffraction experiment "e", at 10 s/step, $25° \leqslant 2\theta \leqslant 40°$

⇓

8 months storage at RT
X-ray diffraction experiment "f", at 20 s/step, $25° \leqslant 2\theta \leqslant 40°$

PW3710 Based diffractometer, Cu K_α radiation Step: 0.020° in 2θ

Total duration of experiments: 39 months

the six original specimens were submitted to a HT at (148 ± 1) °C. Prior to HT, the specimens were lightly abraded again with 2500 emery paper, cleansed in hot ether, rinsed in doubly distilled water, dried in hot air and sealed in an evacuated Pyrex glass tube filled with high purity argon. They were held at temperature for 2212 h and furnace cooled at $v_c \approx 1$ °C/min. The extent of the HT was long enough to assure equilibrium was reached, as predicted by Kearns [27] for 99% homogenization in the two phase region. XRD experiment 'c' was made immediately after HT. As before, metallographic samples were cut from these specimens.

The X-ray beam section is approximately 1 cm^2 and 90% of the diffracted intensity comes from a layer 2–11 μm deep, depending on 2θ. Files number 05-0665 (α-Zr), 34-0690 (γ-ZrH), 34-0649 (δ-Zr hydride) from the Joint Committee on Powder Diffraction Standards (JCPDS) were used for indexing the diffractograms. Semiquantitative calculations of phase proportions – as mass % of hydride in the alloy – were made from the diffractograms 'a' and 'c' ($20° \leqslant 2\theta \leqslant 130°$) using the Rietveld method and software by Lutterotti [28] and considering the texture of the phases. The estimated error of these values is about 30%. For the sake of a better detection of the γ-hydride, which was expected to be formed during the 148 °C HT and RT-aging [3,6–9], some high sensitivity diagrams were made at a speed of several seconds per step (Fig. 1).

3. Results

3.1. Characterization by X-ray diffraction and metallography

All the X-ray diffraction studies (series 'a' to 'f') show a textured hydrogen saturated hcp α-Zr matrix and textured fcc δ-hydride.

The characteristic peaks of the γ-ZrH phase were never detected, neither a few days after autoclaving (series 'a') nor after 19 months storage at room temperature (series 'b'). XRD experiment 'c', made immediately after the 148 °C HT, showed, as before, only α-Zr and δ-hydride. No evidence of the γ-hydride was observed either in the higher sensitivity diagrams made after RT aging (series 'd' to 'f').

The diffractograms of the series 'f' experiments are presented in Fig. 1. Four reflections are seen in all of them, namely, for increasing 2θ, (1 0 0) α-Zr; (1 1 1) δ-hydride; (0 0 2) and (1 0 1) α-Zr, as well as a very weak, highly deformed indication of the δ-(2 0 0) reflection. The relative intensities of the peaks indicate (1 1 1) textured δ-hydrides in a (0 0 2) textured α-Zr matrix. The position of the γ-(1 0 1) and (0 0 2) reflections, respectively, have been marked in the graphs, though these peaks were not observed.

The results of the autoclaving tests and semiquantitative information from XRD experiments are summarized in Table 2. The first three columns show the sample

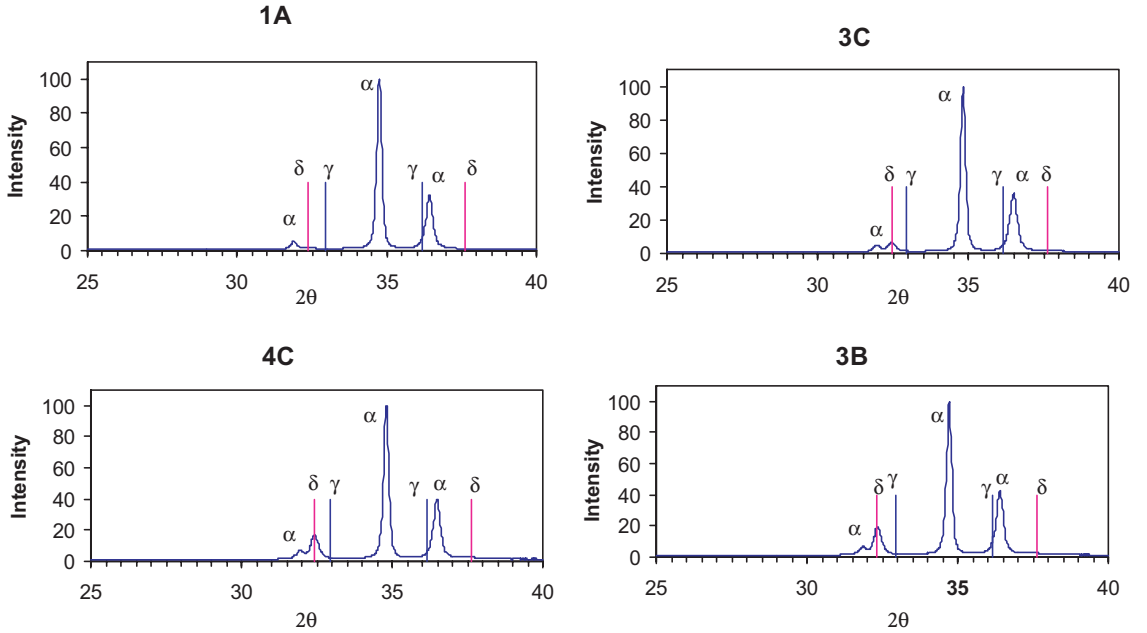

Fig. 1. Diffractograms from XRD experiment 'f', 13 months RT storage after HT at 148 °C. PW3710 Based diffractometer, CuKα radiation step: 0.020° in 2θ. 20 s/step, $25° \leqslant 2\theta \leqslant 40°$.

Table 2
Results from autoclaving tests and XRD experiments

Sample Id	Hydrogen content	Hydrogen content	Mass % δ-hydride prior to HT from XRD	Mass % δ-hydride after HT from XRD	If only delta-hydride had precipitated. Calculated content of delta-hydride, mass %			If only gamma-hydride had precipitated. Calculated content of gamma-hydride, mass %	
Number of steps	C_H (at.%)	C_H (wt ppm)	Series 'a'	Series 'c'	25 °C	148 °C	340 °C	25 °C	148 °C
1A-1	1.6	174 ± 17	1.2	1.5	1.0	1.0	0.4	1.6	1.6
4A-1	3.8	429 ± 43			2.5	2.5	2.0	3.9	3.9
3C-2	4.9	565 ± 56	2.0	3.4	3.3	3.3	2.8	5.2	5.1
4C-2	7.3	870 ± 87	5.0	9.6	5.0	5.1	4.7	8.0	7.9
3A-3	7.0	831 ± 83			4.8	4.9	4.5	7.6	7.6
3B-4	12.1	1516 ± 152	9.7	8.2	8.8	8.9	8.7	13.9	13.8

Calculated mass percent of hydride phases.

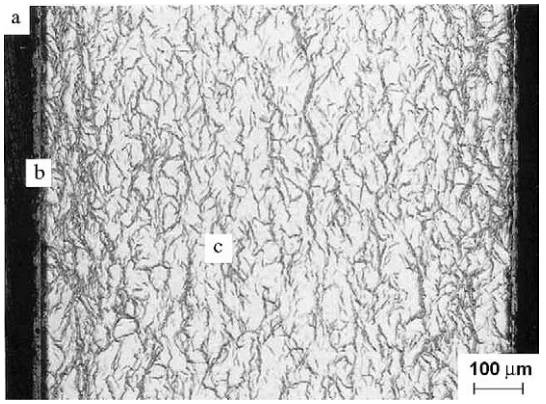

Fig. 2. Optical micrograph of specimen 4C after autoclaving (870 wt ppm H): (a) epoxy resin, (b) oxide layer, (c) δ-hydrides in a Zry-4 matrix. Observe hydride surface layering.

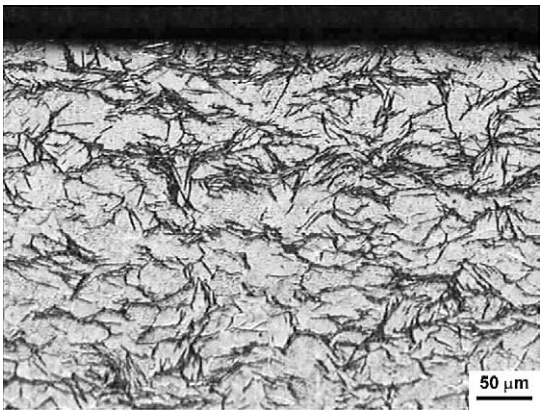

Fig. 3. Optical micrograph of specimen 4C after HT at 148 °C (870 wt ppm H). Inter- and intragranular δ-hydrides in a Zry4 matrix. Hydride surface layering can still be observed.

identification and number of autoclaving steps they were submitted to, and the hydrogen concentration both in

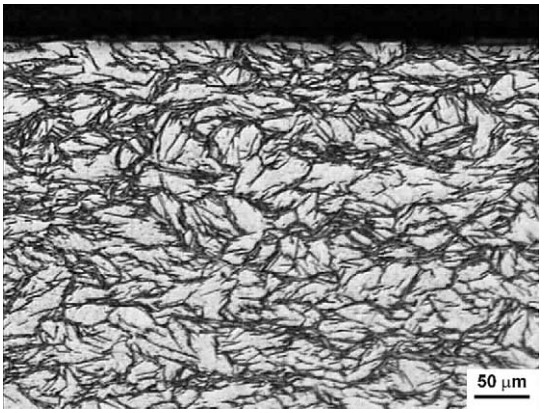

Fig. 4. Optical micrograph of specimen 3B after HT at 148 °C (1516 wt ppm H). Thick distribution of inter- and intragranular δ-hydrides.

atomic % and wt ppm. Columns 4 and 5 contain the estimations of the mass percent of δ-hydride in the alloys, both before the HT and after it (from series 'a' and 'c' diffractograms). The other five columns list the theoretical amounts of the mass % of the δ- and γ-phases, which would be formed according to the Zr–H phase diagram at different temperatures, namely RT, aging HT and autoclaving. For the calculation, the $\alpha/(\alpha+\delta)$ and $(\alpha+\delta)/\delta$ solvi from [2,4] and the $\alpha/(\alpha+\gamma)$ and $(\alpha+\gamma)/\gamma$ solvi from [5,13], respectively, were used. These calculations show that the equilibrium mass percent of γ-hydride is considerably larger than that of δ at the aging temperature. Since our HT was long enough for equilibrium to be reached, the fact that no γ-XRD intensity peak was observed is important.

The amounts of δ-hydride in the specimens immediately after autoclaving increase with hydrogen content, and have not changed after the HT, except for specimen 4C. Fig. 2 shows the inhomogeneous hydride distribution in sample 4C after autoclaving.

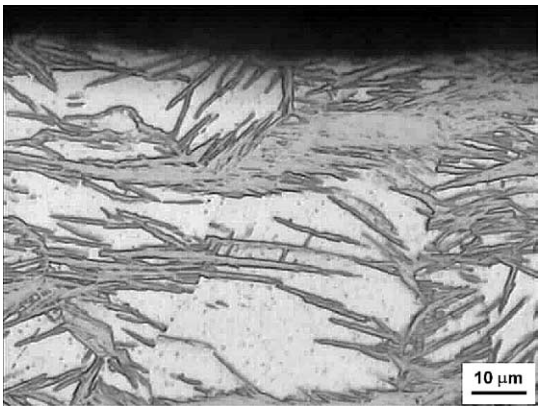

Fig. 5. Higher magnification optical micrograph of specimen 3B after HT at 148 °C. δ-hydride needles and plates can be clearly observed.

The hydride distribution after HT was observed by optical microscopy on cross-sections cut from the samples. Surface hydride clustering is observed in all the samples, to a higher degree in specimen 4C (Fig. 3). The most homogeneous specimen is 3B (1516 wt ppm H), with four autoclaving steps (Fig. 4). Under higher magnifications, the clusters are seen to consist of thin hydride needles, either in parallel arrangements or forming long strips, as illustrated in Fig. 5, from specimen 3B. In general, the micrographic examination showed that the HT produced no significant changes in the appearance and distribution of the hydrides with respect to those after the autoclaving process reported elsewhere [11,12].

4. Discussion

In short, the present results show that in non-etched recrystallized Zircaloy-4, hydrided in autoclave at 340 °C and slow cooled (0.5 °C/min), only δ-hydride is detected by XRD. After aging at RT, at 148 °C and subsequent RT-aging, no evidence of γ-hydride is observed either in these non-etched specimens.

The XRD experiments described here are representative of a surface layer 2–11 μm deep and the relative intensities of the phases are affected by texture, since the diffractograms were made on massive specimens. In spite of these limitations, the amounts of δ-hydride calculated with the Rietveld method compare well with the equilibrium diagram (Table 2). In general, the δ mass % was not affected by the HT, a fact which indicates that no $\delta \rightarrow \gamma$ transformation took place in our material at 148 °C. The changes detected in sample 4C might be due to the initial inhomogeneity of hydride distribution in 4C, which had received only two autoclaving steps (Figs. 2 and 3). No γ-hydride was ever detected, though the amounts predicted in the Zr–H diagram [5] are quite large (Table 2).

The absence of a $\delta \rightarrow \gamma$ transformation after the 148 °C HT will be discussed after analyzing the literature referring to the occurrence of γ- and δ-hydride in zirconium and its alloys.

In order to study the somewhat contradictory results in the literature up to 2002, the authors organized this review according to ideas presented by Cann et al. [14] in their study of the influence of metallurgical factors on the nature of the hydride phase which would precipitate in zirconium with up to 200 wt ppm hydrogen. Cann observed that a higher impurity content, especially about 1000 wt ppm oxygen, favors the formation of δ-hydride, while γ-hydride predominates in materials with about 200 wt ppm oxygen. They studied the influence on the hcp lattice of the strains associated with nucleation and growth of each kind of hydride. Through a simplified model, they point out that due to a lower elastic strain energy, γ-hydrides nucleate on cooling from just above terminal solid solubility (TSS). As hydrides grow, plastic relaxation occurs. At this stage, in hard materials the δ-phase has the lower transformation strain energy, so the original γ-hydrides may transform to δ and continue growing as this phase. For soft materials, which are those with the lower oxygen content, the difference in transformation strain energy between these phases is very small, and consequently the γ-hydride, once precipitated, will continue to grow.

In order to analyze these ideas, entries in Table 3 have consequently been ordered according to the purity of the starting material, quoted in column 3. The amount of hydrogen introduced in the specimens is presented in column 4, while hydriding procedure and subsequent HTs are reported next. The last column describes phases observed after the treatments mentioned in column 5, and, where pertinent, the column has been divided in order to include any further aging and phase evolution. Both dynamic and static studies are presented.

Panel A is devoted to studies of the Zr–H binary system and to solutions of hydrogen in α-zirconium alloys, Panel B to hydrogen in alloys of the Zr–Nb system, including a cooperative TSS study in material from a pressure tube (PT) [8,22,23]. General references to the phase diagram and aging treatments of the Zr–Nb system are taken from [29]. The first seven entries of Panel A summarize results of work on high purity zirconium (>99.9 wt%) while the rest of them refer to less pure zirconium and zirconium alloys.

4.1. High purity zirconium

Mishra et al. [3] and Bashkin et al. [6,7] present XRD and dynamic studies of phase transformations in hydrogen-rich alloys and support the existence of the

Table 3
Literature survey on zirconium hydrides

Material	Author	Purity	H content (110 wt ppm ≈ 1 at.%)	Hydriding procedure and heat treatments	Phases present	
Panel A: Pure zirconium and hcp zirconium alloys						
Zr	[3]	Iodide Zr 99.93% (Hf: 95 ppm; O: 80 ppm)	10 at.%	β-HT → WQ / AC / FC	α-Zr No hydrides α-Zr + 5%δ No γ α-Zr + 10%δ No γ	6.5 months RT-aging: α-Zr + 10% γ No δ (XRD)
			18 at.%	β-HT → FC		2 months RT-aging: partial α + δ → γ transformation on the surface
			4.5 at.%	AN 520 °C (α) → WQ	α + δ + γ	
			44 and 47.5 at.%	β-HT → WQ	α + δ + γ	6.5 months RT-aging: α + γ DTA: change in slope at 255 °C only on heating
Zr-deuteride	[6]	'Very pure Zr' (99.94%)	$ZrD_{1.01}$	Synthesized 800 °C (β or β + δ) + HPT to maximize amount of γ-phase → FC C_p (T) on heating at 3.5 °C/min	Three-phase material (α + δ + γ) α + δ → γ peritectoid at 297 to 367 °C Claim evidence of reversibility of γ → α + δ transf. (from heating cycles beginning at 120 °C) C_p peritectoid <10% C_p eutectoid	
Zr-deuteride	[7]	'Very pure Zr' (99.94%)	$ZrD_{0.99}$ $ZrH_{0.96}$	Synthesized gaseous H or D DTA under pressure 0.1–0.6 GPa Cycling (17–347 °C) XRD	α + γ + δ Thermal effects at $T_p \approx 277$ °C on heating and cooling, blurred after ≈12 cycles Unaffected by very fast heating or cooling rates T_p decreases with pressure	
Zr	[13]	Marz Zr > 99.97% (O: <200 ppm)	4, 8, 12, 21, 99, 160, 230 ppm Determines solvus α/γ and α/(γ + δ)	Gaseous hydriding + Hom 800 °C (α, 3 days) → FC + HT at 140 °C ⩽ T ⩽ 470 °C → WQ (TEM and OM)	$C_H \leqslant 21$ ppm, $T \leqslant 250$ °C, solvus α/γ. $C_H \geqslant 99$ ppm, 366 °C ⩽ T ⩽ 420 °C, solvus α/(γ + δ)	C_H: 21 and 99 ppm, 2 weeks 200 °C aging → FC: α+ only γ-hydride
Zr	[14]	Marz Zr > 99.97% (O: <200 ppm)	13, 31, 108, 170 ppm	Hom 800 °C (α, 3 days) → FC	Both HT: $C_H \approx 15$ ppm: α+ only untwinned γ-needles $C_H \approx 30$ ppm: α+ only twinned and untwined γ $C_H > 100$ ppm: α+ twinned γ+ isolated grains of δ (TEM)	
			16, 32, 113, 180 ppm	Hom 450 °C (α, 7 days) → FC		
Zr	[15]	Iodide 99.93% Zr (Hf: 95 ppm; O: 80 ppm)	4–13 at.%	Gaseous charging, at $T >$ 700 °C (α + β) → WQ	Martensite α′ + internally twinned γ-plates Possible sequence during WQ: α + β → α′ + β_{enr} → α′ + γ (shear transformation)	
Zr	[16]	Zr > 99.9% (O: 500 ppm)	$ZrH_{1.27}$ bars of hydride	Hydriding at 800 °C (β + δ) + 12 h AN at 500 °C (α + δ) → FC	δ-matrix + α-Zr + twinned γ-platelets	6 months RT-aging: increase of γ at α/δ interfaces (XRD, OM)

Zr	[17]	Sponge Zr 99.8% (O: 1300 ppm) OM and TEM	200 ppm (1.78 at.%)	Hom 454 °C (α, 30 min) → WQ	α + intragranular γ-hydrides	1 week 200 °C-aging → WQ α + intergranular δ-hydrides
			500 ppm (4.33 at.%)	Hom 535 °C (α, 30 min) → IBQ	Intra + intergranular γ-hydrides + α	3 weeks 200 °C aging → WQ α + intra + intergranular δ-hydrides
						3 weeks 150 °C aging → WQ α + intragranular γ + few intergranular δ-hydrides
				Hom 535 °C (α, 30 min) → FC down to 200 °C		3 weeks 200 °C aging → WQ α + thick intra and intergranular δ-hydrides
				Hom 535 °C (α, 30 min) → FC down to RT	α + thick intra and intergranular δ-hydrides	
Zr	[14]	Reactor grade Zr 99.8% (O: 1380 ppm) Commercial Zr 99.7% (O: 1250 ppm)	29, 42, 110, 120 ppm 27, 51, 109, 119 ppm ≈25, 64, 100, 200 ppm	Hom 800 °C (α, 3 days) → FC Hom 450 °C (α, 7 days) → FC Same HTs	TEM All materials, all HT: $C_H < 50$ ppm: α + δ + γ $C_H > 100$ ppm: α + only δ-hydride	
Zr	[10]	Zr ≈ 98.75% (Cr: 1.15%, Fe: 0.1%, O: ⩾1000 ppm)	24 ppm Up to 4200 ppm (27.5 at.%)	Air cooling no – T mentioned Hydrided in steam at 500 °C (α + δ, 334 days) → CR: 1–2 °C/min down to RT	TEM: α + acicular γ-hydrides TEM and XRD: α + large globular δ	2200 h 240–220 °C aging: α + large globular δ-hydrides No evidence of δ → γ transformation either in globules or at α/δ interface
Zr	[18]	Zr > 97.51% (Hf: 2.40%, O: 100 ppm, Fe: 400 ppm)	$ZrH_{0.1}$	Hom (100 °C, 21 h)	α + δ + traces of γ	
			$ZrH_{0.15}$	Hom (125 °C, 20.5 h)	α + δ + traces of γ	
			$ZrH_{0.25}$	Hom (150 °C, 20 h)	α + δ + traces of γ	
			$ZrH_{0.53}$	Prep. at 150 °C No hom	α + δ + small amount of γ	
			$ZrH_{1.10}$	Hom (175 °C, 15.5 h)	α + δ + small amount of γ	
			$ZrH_{1.33}$	Hom (225 °C, 20.5 h)	α + δ + traces of γ	
			$ZrH_{1.44}$	Hom (225 °C, 19 h)	δ + traces of γ	
Zr	[19]	Commercial Zr (O: ⩾1000 ppm)	$ZrH_{0.4}$ to $ZrH_{1.0}$	Hydriding at 600 °C (β or β + δ) → FC	α, δ, γ, all present in large quantities	
			$ZrH_{0.4}$ to $ZrH_{1.0}$	Hydriding at 900 °C (β or β + δ) → FC	Large δ grains in α -Zr matrix	
			$ZrH_{1.0}$ to $ZrH_{1.5}$	Hydriding at 900 °C (β or β + δ) → FC	Primary δ, secondary γ, some α	
Zr	[20]	Sponge Zr (O: 1300 ppm, N: 80 ppm)	100, 250, 600 ppm		Metallography and XRD All Hydrogen contents:	
				• Hydriding at 550 °C (α) → WQ	• α + almost exclusively γ	
				• Hydriding at 550 °C (α) → AC	• α + Widmanstatten needles of δ and γ-hydrides	
				• Hydriding at 550 °C (α) → FC	• α + mainly intergranular δ-hydride, (in 600 ppm H, also needles of γ within δ-phase and intragranular γ in α-Zr-matrix)	

Table 3 (*continued*)

Material	Author	Purity	H content (110 wt ppm ≈ 1 at.%)	Hydriding procedure and heat treatments	Phases present
Zry-2	[21]	Nuclear grade Zry-2 (1400 ppm O max)	50, 70, 100, 250, 550, 1150 ppm	Autoclave hydriding in 0.5 M LiOH at 300 °C $\leqslant T \leqslant$ 360 °C ($\alpha + \delta$)	XRD: hydrides not detected TEM: $C_H < 100$ ppm: α + mostly twinned γ-hydrides + some plates of δ $C_H > 100$ ppm: α + mostly δ + some γ
Zry-4	Present work	Nuclear grade Zry-4 (1400 ppm O max)	174, 565, 870, 1516 ppm	Autoclave hydriding in 1M LiOH at 340 °C ($\alpha + \delta$) → CR ≈ 0.5 °C/min down to RT	No etching XRD: All hydrogen contents: α + only δ-hydrides All hydrogen contents: 2 years RT-aging: α + only δ + 3 months 148 °C: α + only δ + 1 year RT-aging: α + only δ
			H content		
Panel B: Zr–Nb					
Zr–2.5Nb Cooperative TSS study	[22]	PT Zr–2.5%Nb	0.2, 0.5, 1.0, 2.0 at.% H and 1.0 at.% D	Gaseous charging + 3 days vacuum HT at 400 °C ($\alpha + \beta_{enr} + \omega$) Hydrided mat.: → FC Deuterided mat: → IBQ or FC	Study hydride orientation, and TSS by SANS and metallography No discussion of type (δ or γ) of hydride precipitates
	[23]	PT Zr–2.5%Nb	D: up to 100 ppm equiv H (0.9 at.% H)	Electrolytic deuteriding at 90 °C + Hom at Kearrns' TSSD Internal friction at heating and cooling rates 2 °C/min	TSS as function of T_{max} No discussion of γ/δ For $C_H = 79$ ppm, two humps can be observed at $T \approx 240$ °C and 180 °C in $\delta E/\delta T$ in heating and cooling
	[8]	PT Zr–2.5%Nb (O: 1060 ppm, N: 23.5 ppm, H: 8.5 ppm)	(0.70 D + 0.08H) at.% (D + H) = 0.44 at.%	Electrolytic deuteriding + Hom 360 °C, 60 h ($\alpha + \beta_{enr} + \omega$) (large hydrides) TSS by SANS at 2.5 °C/min Heating runs: 37–407 °C Soaking at 407 °C Cooling runs to 37 °C	First heating run: γ-(dominant) and δ-hydrides, at $T > 200$ °C: γ not detected, at 407 °C: no hydrides On cooling from 407 °C: γ-intensities reported at 320 degrC > $T > 220$ °C Second heating run: γ (halved) and δ-hydrides, at $T > 200$ °C: γ not detected, at 407 °C: no hydrides δ/γ transformation at $T \approx 180$ °C suggested
Zr–2.5Nb	[9]	PT Zr–2.5%Nb (O: 1060 ppm, N: 23.5 ppm, H: 8.5 ppm) Is there a slow δ/γ-phase transformation?	200 ppm D (≈100 ppm H)	Gaseous charging at 400 °C + AN at 450 °C 72 h Hom 750 °C 1 week $(\alpha + \beta)_{Zr}$ Soaking at 450 °C ($\alpha + \beta_{enr} + \omega$) → HQ to 180 °C → FC to 17 °C	Neutron diffraction (ND) at 450 °C (no hydrides) ND study of transformation kinetics at 17 °C over a period of 60 h Results: Amount of γ at 17 °C: $I_\gamma = a \cdot t^{0.22}$ Amount of δ remains constant
Zr–2.5Nb	[24]	PT Zr–2.5%Nb	60 ppm H	Electrolytic hydriding DHC testing at 250 °C (test duration not reported)	XRD, texture analysis at: • 20 mm from fractured surface: no hydrides reported, though low intensity (1 0 1) γ can be seen in Fig. 7 [24] • fracture surface: only reoriented δ-hydrides on α-Zr

Zr–2.5Nb	[19]	PT Zr–2.5%Nb	$ZrH_{0.1}$ to $ZrH_{1.0}$	Hydriding at 600 °C (α, $\alpha+\beta$, β or $\beta+\delta$) → FC or WQ	α, δ and some γ
			$ZrH_{0.1}$ to $ZrH_{1.0}$	Hydriding at 900 °C (β or $\beta+\delta$) → FC	Matrix α, fine δ-hydride distribution
			$ZrH_{1.0}$ to $ZrH_{1.5}$ (TEM)	Hydriding at 900 °C (β or $\beta+\delta$) → FC	Primary δ, secondary γ, some α some Nb ppts
Zr–5Nb Zr–10Nb Zr–20Nb	[25]	Arc-melted reactor grade Zr and Nb	13 at.% $\leqslant C_H \leqslant$ 63 at.%	Study solvus $\beta/(\beta+\delta)$ and $(\beta+\delta)/\delta$ at 700 °C $\leqslant T \leqslant$ 900 °C. Experimental P-C isotherms	Increasing Nb content, diminish H solubility in the β and δ phases and increases the equilibrium H pressure for any fixed concentration of H. In the presence of Nb, precipitation of δ-hydride from saturated β-Zr is unfavorable. No mention of γ
Zr–20Nb	[15]	Zr–20%Nb	• 520 ppm H • 85 ppm H	• Chemical etching at RT • Electropolishing (EP) (−50 °C)	In a β-matrix, γ-precipitation induced by chemical etching and electropolishing
			• 335 ppm H (XRD, TEM, ED)	• 800 °C Hydriding (β_{Zr}) → WQ	Internally twinned γ-hydride plates precipitate in a β matrix on WQ to RT. (shear transformation)
Zr–19Nb	[26]	Nuclear grade Zr and Nb 99.99%	H introduced by etching and EP (very low C_H)	Etching: HNO_3, HF, H_2O (RT) Electropolishing (−50 °C)	TEM: twinned γ-hydrides XRD: fct structure $a = 4.50$ Å, $c = 5.22$ Å

IBQ: Iced brine quenching; WQ: Water quenching (100 °C/s); AQ: Air quenching; HQ: Helium quenching (15 °C/min); AC: Air cooling (≈6 °C/min); FC: Furnace cooling (1–3 °C/min); HPT: Heat and pressure treatments; AN: Annealing; Hom: Homogenization; CR: Cooling rate.

peritectoid reaction $\alpha+\delta \rightarrow \gamma$. Their experimental evidence can be summarized as follows: Mishra et al. [3] report a change in the slope of the DTA curve at 255 °C on heating $(\alpha+\gamma)$-Zr44.5at.% H, but not on cooling, and suggest a sluggish peritectoid reaction occurs at that temperature. Similar effects at higher temperatures, in the range 297 °C $< T <$ 367 °C, were observed by Bashkin in his calorimetric heating curves of $ZrD_{1.01}$ [6], and with DTA both on heating and cooling $ZrH_{0.96}$ under pressure [7]. The DTA peaks became blurred in successive cycles and the effect finally disappeared. These successive cycles were made at different pressures, in the range 0.1 to 0.59 GPa, and the experimental peritectoid temperature at atmospheric pressure is actually not reported in [7]. Mishra et al. point out that the extent of the peritectoid reaction is dependent on the amount of α/δ interfaces [3].

Barraclough and Beevers [16] investigated as well the hydrogen-rich region of the diagram, and present XRD and metallographic evidence of γ formation in δ/α interfaces after 6 months RT-aging high purity $ZrH_{1.27}$.

Results by Cann and Atrens [13] and Cann et al. [14] on dilute alloys of hydrogen in Marz zirconium (>99.97% pure) support the existence of a peritectoid reaction at 250 °C in agreement with Mishra et al. [3]. The presence of only γ-hydride after 2 weeks 200 °C aging [13] does not agree with the δ/γ transformation at 180 °C suggested by Root and Fong in Zr–2.5%Nb [8].

Dey and Banerjee studied iodide zirconium with up to 13 at.% H [15] and proposed that on quenching from the β or $(\alpha+\beta)$ regions, γ is formed from the hydrogen enriched β-phase by a shear mechanism.

In general it can be observed that γ-phase predominates in Zr–H alloys prepared with high purity zirconium (>99.9% Zr), the amount of γ increasing after aging at RT or at about 200 °C.

4.2. Low purity zirconium

Since the $\alpha/(\alpha+\gamma)$ solvus at $T = 286$ °C is $C_H = 47$ wt ppm [5] or 33 wt ppm [13], the coexistence in low purity zirconium of γ- and δ-hydrides at $C_H < 50$ wt ppm [14] would contradict the possibility that γ be an equilibrium phase, while the observation by Northwood of only γ-hydride at $C_H = 24$ wt ppm in zirconium containing Fe and Cr [10] would support it. Results by De et al. in autoclaved Zircaloy-2 [21] are no concrete evidence of the peritectoid reaction $\alpha+\delta \rightarrow \gamma$ because in their work, as well as in Northwood's, only TEM is used for hydride characterization, while Gill et al. [20] have observed that TEM results might be unreliable in the absence of confirmatory XRD work. It is also not clear why no hydrides were detected by De at $C_H > 100$ wt ppm by XRD, while in the present work hydrides were detected by this technique.

HT of low purity zirconium do not in general support the peritectoid reaction proposed by Mishra, Bashkin or Root [3,6–9]. As an example, after aging at about 200 °C [10,17] only δ-hydrides are reported, whichever the primary hydride type be. Our long term aging at about 150 °C of Zircaloy-4 samples containing only primary δ-hydrides showed no evidence of γ, while after short term 150 °C aging of samples containing only primary γ-hydrides [17] partial $\gamma \rightarrow \delta$ transformation was reported. HT by Gulbransen at $T < 180$ °C in zirconium with 2.4 wt% Hf (α-stabilizer) [18] do not support the transition either. The treatments in [17,18] were probably too short to achieve equilibrium at such a low temperature. However, these results indicate that no phase transition takes place at 180 °C in low purity zirconium and Zircaloy-4.

Results for higher hydrogen content are rather contradictory. For instance, Gulbransen and Andrew [18] report that in $ZrH_{1.44}$ homogenized at 225 °C, δ and traces of γ are detected, which would support the peritectoid, while in $ZrH_{1.33}$ homogenized at 225 °C for a slightly longer period, the α-phase is observed together with δ and traces of γ, a result which is not in agreement with the peritectoid. Though results by Simpson and Cann [19] on commercial grade zirconium with $1.0 \leqslant H/Zr \leqslant 1.5$ do not discard the peritectoid reaction $\alpha + \delta \rightarrow \gamma$, the phases reported at $0.4 \leqslant H/Zr \leqslant 1.0$ do not support it either.

Beck [1] studied samples of Zr–H (purity of the zirconium is not reported) in the composition range $0.98 \leqslant H/Zr \leqslant 1.49$ aged at temperatures in the range 400–600 °C and cooled at different rates. He observed that the amount of γ-phase which is formed remains constant and is independent of the hydrogen content. As a fast γ-formation kinetics is observed, he further proposes a diffusion-controlled twinning process similar to that encountered in the formation of Fe–C martensite for γ-precipitation from δ-hydride.

The effect of cooling rate on hydride phases in low purity zirconium is studied by Gill et al. [20] in good agreement with results by Nath et al. [17]. These results would show an increase in the amount of γ-phase with increasing cooling rate, as opposed to Mishra's results. The exclusive presence of γ-phase in quenched specimens would indicate a fast formation kinetics, not in agreement with the nature of peritectoid reactions, which are sluggish and incomplete.

4.3. Zirconium–niobium

The first four entries in Panel B of Table 3 present work on Zr–2.5%Nb. A cooperative investigation of the TSS of dilute solutions of hydrogen in Zr–2.5%Nb by Fong using SANS [8,22] and Pan using internal friction [23] is particularly interesting. In [22,23] emphasis is put in the study of TSS for dissolution and precipitation by two different dynamic methods, and hysteresis is discussed, while no comments on the type of hydrides are made. However, in Fig. 4 of [23] (TSS determination from the derivative of Young's modulus E vs temperature) two small humps can be observed on the $\delta E/\delta T$ vs T curve for 79 wt ppm H both on heating and on cooling at about 180 and 240 °C. This peculiarity of the curves, notably similar to the 'effects' reported by Bashkin et al. [6], is however not discussed by the authors.

In a later work, Root and Fong [8] and Small et al. [9] continue their TSS studies by SANS with a characterization of the hydride phases. From heating, soaking and cooling experiments a $\delta \rightarrow \gamma$ transformation at 180 °C is proposed in [8]. In their plot of the intensity of the γ- and δ-peaks vs temperature on heating (Fig. 8 of [8]), a decrease of γ-intensity and an increase of that of δ are observed at $T \approx 180$ °C. However, on cooling after 2 h soaking at 407 °C ($T > TSS$) (Fig. 9 of [8]), γ-intensities are also reported in the range 220 °C $< T <$ 320 °C, well above the transition temperature they propose. It is not apparent that below 180 °C growth of γ proceeds at the expense of δ. The amount of γ produced after cycling is always smaller than the original amounts, in coincidence with Bashkin et al. [7]. Small et al. [9] report an exponential increase of the amount of γ-hydride in Zr–2.5%Nb with 200 wt ppm deuterium during RT aging, while the amount of δ remains constant.

Kim et al. [24] studied the influence of hydrides in the fracture of Zr–2.5%Nb from pressure tubes. They report XRD evidence of (1 1 1) textured δ-hydrides in the crack tip region after DHC tests at 250 °C.

Some results from hydrogen rich PT Zr–2.5%Nb by Simpson and Cann [19] might support the peritectoid, except for samples with $0.1 \leqslant H/Zr \leqslant 1.0$ hydrided at 900 °C, in which no γ is detected.

Alloys in the Zr–Nb system being dual phase materials, small amounts of bcc β-Zr–20%Nb phase can be present in Zr–2.5%Nb. Some results from Zr–20%Nb, from Dey et al. [15,26] are also presented in Panel B of Table 3. They observed γ-precipitation both after quenching material which had been hydrided in β and after chemical etching or electropolishing at low temperatures non-hydrided material. Dey infers that hydrogen released during those procedures diffuses into the β-Zr-lattice and produces the γ-hydride through a shear transformation resulting in the change from bcc to the fct structure. Experimental results by Sinha and Singh [25] show that δ-hydride precipitation in hydrogen saturated β-Zr is unfavorable in the presence of niobium.

4.4. Concluding remarks

In short, the review shows that in lower purity zirconium (<99.8 wt%) as well as in hcp-zirconium alloys experimental evidence does not support the stability of the γ-phase nor the existence of a peritectoid reaction, while in higher purity zirconium there is experimental

evidence of such a reaction at about 250 °C. Hydrided Zr–2.5%Nb alloys from pressure tubes also undergo some kind of transformation in the range 170 °C < T < 220 °C.

Our results in Zircaloy-4 are in good agreement with the results for low purity α-zirconium reported in the literature. In general, γ-hydride does not seem to be an equilibrium phase whenever α-stabilizers (O, Hf, Sn) are present. However, in the higher purity materials in which the amounts of these α-stabilizers are extremely low, γ-hydride is apparently an equilibrium phase.

Niobium is a β-stabilizer in zirconium. Actually, Dey and Banerjee [26] point out that even dilute alloys, like PT Zr–2.5%Nb in the (α + β) extruded condition, contain a substantial volume fraction of the β-phase containing 10–20% Nb. They report that in bcc-β materials, γ-hydrides are observed in preference to δ [15,26]. It is not clear whether Root [8,9] has considered the preferential precipitation of the γ-phase in β when they report their 180 °C and RT δ → γ transformation. A comparison between the dynamic studies by Bashkin et al. [6,7] and those by Root shows that the shape of the curves smoothes down after a number of successive heating and cooling cycles. This phenomenon must somehow be related to the nature of the transformation. A true comparison of the results in Zr–Nb and those by Bashkin and Mishra could actually be made only after a study of the ternary Zr–Nb–H system.

Some theoretical studies of the Zr–H system recently published are those by Ma et al. [30] and by Domain et al. [31]. Work by Ma [30] is a theoretical qualitative investigation of γ-hydride precipitation in a zirconium bicrystal. Domain [31] performs an ab initio study of the bulk properties of the Zr–H system, and points out that the nearly equal formation energies of the three hydrides indicate that their relative stabilities probably depend on mechanical and thermal contributions to the free energies and may thus be modified by slight variations of the parameters involved in thermomechanical treatments.

Some of the results reported in the literature up to 2002 seem to be contradictory. The apparent contradictions might well be pointing at the theoretical result mentioned above, and that mechanical properties of the lattice would be most important for the type of hydride that would precipitate, as already suggested by Cann in his 1984 study of the strengthening effect of impurities [14].

5. Conclusions

Only δ-hydride is detected by XRD after autoclave hydriding Zircaloy-4 at 340 °C in LiOH for $C_H > 100$ wt ppm. Chemical etching was avoided throughout.

Within the detection limit of XRD, none of the characteristic diffraction peaks of the γ-hydride were observed either after autoclaving or after aging at 148 °C and RT.

The literature shows experimental evidence that γ-hydride is an equilibrium phase in high purity zirconium, while in less pure zirconium and α-zirconium alloys γ-hydride is a metastable phase.

The presence of α-stabilizers favors the growth of δ-hydride (hardening effects).

Nuclear grade Zircaloy-4 should contain principally δ-hydride as a stable phase.

The anomalies in the dynamic studies in Zr–2.5%Nb might be related to similar effects reported in high purity zirconium.

A study of the ternary system Zr–Nb–H might help in the analysis of the stability of hydride phases in zirconium–niobium alloys.

Acknowledgements

The authors gratefully thank Dra. M. Ortiz Albuixech for her advice, discussions of the diffractograms and the application of Rietveld method, C. di Grillo for the diffractograms, Mag. Ariel Perotti and P. Coronel for specimen preparation and characterization, Dra. D. Arias for her advice, and the support of CNEA.

References

[1] R.L. Beck, Trans. ASM 55 (1962) 542.
[2] D.O. Northwood, U. Kosasih, Int. Met. Rev. 28 (2) (1983) 92.
[3] S. Mishra, K.S. Sivaramakrishnan, M.K. Asundi, J. Nucl. Mater. 45 (1972/73) 235.
[4] E. Zuzek, J.P. Abriata, A. San-Martin, F.D. Manchester, Bull. Alloy Phase Diagrams 11 (4) (1990) 385.
[5] E. Zuzek, J.P. Abriata, A. San-Martin, F.D. Manchester, in: F.D. Manchester (Ed.), Phase Diagrams of Binary Hydrogen Alloys, ASM International, Materials Park, Ohio, 2000, p. 309.
[6] I.O. Bashkin, V.Yu. Malyshev, M.M. Myshlyaev, Sov. Phys. Solid State 34 (7) (1992) 1182.
[7] I.O. Bashkin, A.I. Latynin, V.Yu. Malyshev, Sov. Phys. Solid State 37 (4) (1995) 1146.
[8] J.H. Root, R.W.L. Fong, J. Nucl. Mater. 232 (1996) 75.
[9] W.M. Small, J.H. Root, D. Khatamian, J. Nucl. Mater. 256 (1998) 102.
[10] D.O. Northwood, J. Less-Common Met. 48 (1976) 173.
[11] A. Perotti, L. Lanzani, J.A. Marengo, M. Ruch, Insight 42 (9) (2000) 597.
[12] A. Perotti, L. Lanzani, P. Coronel, M. Ruch, Insight 43 (5) (2001) 323.
[13] C.D. Cann, A. Atrens, J. Nucl. Mater. 88 (1980) 42.
[14] C.D. Cann, M.P. Puls, E.E. Sexton, W.G. Hutchings, J. Nucl. Mater. 126 (1984) 197.
[15] G.K. Dey, S. Banerjee, P. Mukhopadhyay, J. Phys.-C4 43 (1982) C4-327.

[16] K.G. Barraclough, C.J. Beevers, J. Less-Common Met. 35 (1974) 177.
[17] B. Nath, G.W. Lorimer, N. Ridley, J. Nucl. Mater. 49 (1973/74) 262.
[18] E.A. Gulbransen, K.F. Andrew, J. Electrochem. Soc. 101 (1954) 474.
[19] L.A. Simpson, C.D. Cann, J. Nucl. Mater. 87 (1979) 303.
[20] B.J. Gill, P. Cotterill, J.E. Bailey, J. Less-Common Met. 39 (1975) 189.
[21] P.K. De, J.T. John, S. Banerjee, T. Jayakumar, M. Thavasimuthu, B. Raj, J. Nucl. Mater. 252 (1998) 43.
[22] R.W.L. Fong, S. Spooner, Scr. Metall. Mater. 30 (1994) 649.
[23] Z.L. Pan, I.G. Ritchie, M.P. Puls, J. Nucl. Mater. 228 (1996) 227.
[24] Y.S. Kim, Y. Perlovich, M. Isaenkova, S.S. Kim, Y.M. Cheong, J. Nucl. Mater. 297 (2001) 292.
[25] V.K. Sinha, K.P. Singh, Metall. Trans. 3 (1972) 1581.
[26] G.K. Dey, S. Banerjee, J. Nucl. Mater. 125 (1984) 219.
[27] J.J. Kearns, J. Nucl. Mater. 27 (1968) 64.
[28] L. Lutterotti, P. Scardi, J. Appl. Crystallogr. 25 (1992) 459.
[29] S.A. Aldridge, B.A. Cheadle, J. Nucl. Mater. 42 (1972) 32.
[30] X.Q. Ma, S.Q. Shi, C.H. Woo, L.Q. Chen, Scr. Mater. 47 (2002) 237.
[31] C. Domain, R. Besson, A. Legris, Acta Mater. 50 (2002) 3526.